ISSN 1063-7826, Semiconductors, 2024, Vol. 58, No. 4, pp. 302–305. © Pleiades Publishing, Ltd., 2024.
Russian Text © The Author(s), 2024, published in Fizika i Tekhnika Poluprovodnikov, 2024, Vol. 58, No. 1, pp. 3–6.
English Text © Ioffe Institute, 2024.

Surface Morphology of AlN Layers Grown on a Nano-Structured SiN_x/Si(100) Template

V. N. Bessolov[a], E. V. Konenkova[a,*], S. N. Rodin[a], and A. V. Solomnikova[b]

[a] *Ioffe Institute, St. Petersburg, 194021 Russia*

[b] *St. Petersburg State Electrotechnical University "LETI," St. Petersburg, 197022 Russia*

**e-mail: lena@triat.ioffe.ru*

Received February 7, 2024; revised February 28, 2024; accepted February 28, 2024

Abstract—The morphology of ALN layers grown by Metalorganic Chemical Vapor Deposition on nano-structured NP-Si(001) substrates coated with SiN_x has been studied using atomic force microscopy. The AlN layers grown on the SiN_x/NP-Si(100) template demonstrate a surface roughness 3.8 times less than those obtained on NP-Si(100), and are close to the roughness value for the AlN layer grown on a flat Si(111) substrate. It has been proposed a model to explain the differences in the formation of the surface morphology of AlN layers on the NP-Si(100) substrate and the SiN_x/NP-Si(100) template.

Keywords: aluminum nitride, silicon nitride, nano-structured silicon substrate

DOI: 10.1134/S1063782624040031

1. INTRODUCTION

Owing to a unique combination of features, AlN has attracted a great deal of attention in recent decades. Its wide band gap (6.2 eV) lends this semiconductor a high breakdown voltage, fine thermal conductivity, and a large piezoelectric constant; it also has strong potential for application in high-power electronic [1], ultraviolet photonic [2], and acoustic [3] semiconductor devices. Since bulk substrates are limited in size and costly, AlN layers are normally grown on foreign substrates, such as sapphire and silicon (Si) [4]. Their large size and the potential for integration of gallium-nitride and silicon electronics [5] are the key advantages of silicon substrates.

However, it is rather hard to grow high-quality AlN on Si substrates. First, a large lattice mismatch (~19%) between AlN and Si(111) normally results in high densities of threading dislocations and an initial tension stress. Second, a huge mismatch between the coefficients of thermal expansion (~43%) of AlN and Si leads to cracking in the process of cooling the structure from the epitaxy temperature to room temperature [6]. These are the reasons why the thickness of AlN layers grown on Si is normally below 1 μm and is insufficient to suppress dislocations from the hetero-interface [7]. It has been proposed in recent years to perform AlN heteroepitaxy on Si(100) substrates, which are the ones used most widely in silicon electronics, with their surface patterned in the form of rectangular or triangular ridges of micrometer or nanometer dimensions [8]. When forming a structured surface, one may expose planes Si(111) and Si($\overline{1}\,\overline{1}1$) after the deposition of a mask and chemical etching and grow layers at a certain angle (e.g., 54°). Semipolar ($10\,\overline{1}1$) layers on a silicon substrate may be fabricated this way [8].

Thin buffer SiN_x layers are formed on flat silicon or sapphire substrates in advance to improve the quality of AlN layers. Specifically, the use of a buffer SiN_x-layer helped reduce the density of basal-plane stacking faults in epitaxy of semipolar AlGaN($11\overline{2}2$) on a flat m-Al_2O_3 substrate [9, 10].

It was established that SiN_x may exist in several crystallographic variations. Modification β-Si_3N_4 is known to be the most stable [11] and is characterized by a hexagonal unit cell with lattice parameters $a = b =$ 7.63 Å, $\alpha = 60°$, and $c = 2.91$ Å [12], which is used efficiently in selective epitaxy of GaN layers on a sapphire substrate [13].

In the present study, we compare the surface morphology of AlN layers grown by metalorganic chemical vapor deposition (MOCVD) on flat Si(111) substrates and V-shaped nanostructured Si(100) substrates with and without a deposited nanometer buffer SiN_x-layer.

2. PROCEDURE

Nanostructured substrates were fabricated as in [14]. Embryo waves with a small (nanometer) amplitude formed under bombardment of the surface of a

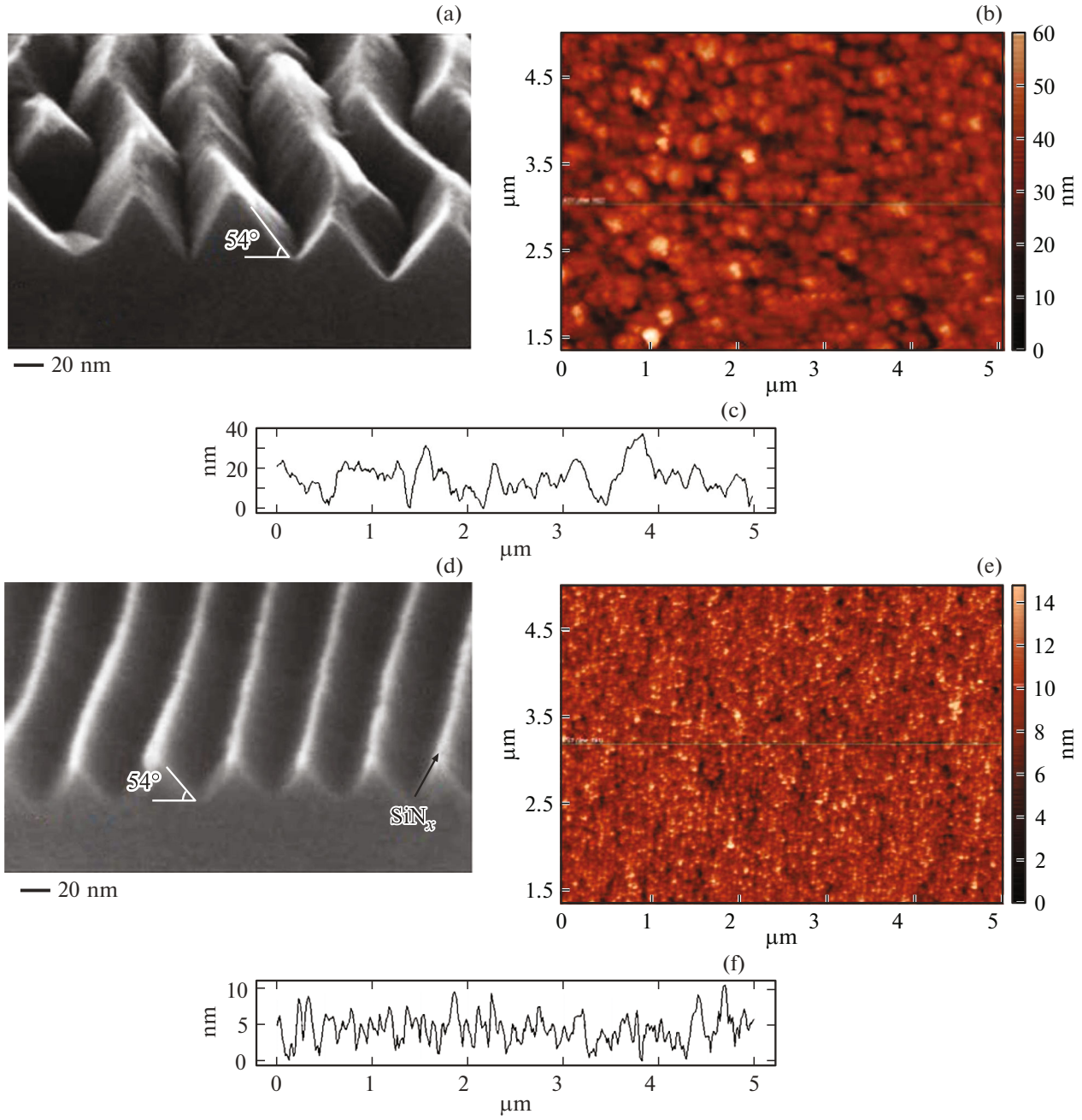

Fig 1. SEM images: (a) NP-Si(100) substrate, (d) Si_3N_4/NP-Si(100) template; AFM images and surface profiles of structures: (b, c) AlN/NP-Si(100), (e, f) AlN/Si_3N_4/NP-Si(100).

silicon substrate by nitrogen ions [14]. Substrates with a nanostructured NP-Si(100) surface (see Fig. 1a) then formed in the process of chemical caustic etching, and templates SiN_x/NP-Si emerged after bombardment of NP-Si(100) by a flux of N^+. It is evident that bright SiN_x strips with different thicknesses of SiN_x at the apex and on the slopes are positioned at the tops of nanoridges of templates (see Fig. 1d).

AlN layers were grown on NP-Si(100), SiN_x/NP-Si(100) templates, and flat Si(111) substrates with a thickness of ~200 nm by MOCVD as in [15]. Sample surfaces were examined with a SolverNEXT scanning probe microscope. AlN layers were grown on a flat Si(111) substrate and on NP-Si(100) substrates with a *V*-shaped profile with ridges ~40 nm in height and Si(111) and Si($1\bar{1}\bar{1}$) faces of two types: uncoated (see Fig. 1a) and coated with SiN_x (Fig. 1d).

Table 1. Root-mean-square (RMS) and average (RA) roughness values of AlN layers grown on different substrates

Substrate template	Root-mean-square roughness (RMS), nm	Average roughness (RA)
Si(111)	1.996	1.470
NP-Si (100)	8.574	6.726
SiN_x/NP-Si(100)	2.214	1.757

3. RESULTS AND DISCUSSION

Panels a–f of Fig. 1 show the topographic features of AlN surface morphology in AlN/NP-Si(100) and AlN/Si_3N_4/NP-Si(100) heterostructures. These features indicate that the surface of AlN grown on the template is smoother than the surface of AlN on NP-Si(100). The root-mean-square (RMS) and average (RA) roughness values of AlN layers grown on the Si(111) substrate, the nanostructured NP-Si(100) substrate, and the SiN_x/NP-Si(100) template are lusted in Table 1.

It is evident that the RMS and RA values of the layer grown on Si(111) are close to the corresponding values of layers on the template (see the table) and differ from the RMS and RA levels of the layer fabricated on NP-Si(100).

As is known, the initial V/III ratio specifies the polarity and morphology of the surface in MOCVD epitaxy of AlN layers. AlN layers grown at high initial V/III ratios have *N*-polarity and a rough surface, while those grown at low initial V/III ratios feature Al polarity and a smooth surface [16]. The V/III ratio in our experiments remained constant in the process of growth of layers of substrates and the template.

We attribute the variation of surface morphology to differences in the surface diffusion length of atoms on the nanostructured substrate and the template. Indeed, surface diffusion length λ_s may be expressed in terms of adsorption energy barrier E_{ad} and diffusion potential energy barrier E_d [17]:

$$\lambda_s = \lambda_e e^{\frac{E_{ad}-E_d}{2k_BT}}, \quad (1)$$

where k_B is the Boltzmann coefficient and λ_e is the effective jump distance on the surface or the distance between two neighboring lattice sites.

The (E_{ad}–E_d) value is 0.55 eV/atom for a Si(111) surface and 0.62 eV/atom for a Si(111) surface coated with Si_3N_4 [18]. It follows from these data that λ_s on SiN_x/NP-Si(100) should be greater than on NP-Si(100) in the course of formation of an AlN seed on substrate and template faces. This should facilitate growth in the region of template nanogrooves and result in a reduction in the average relief height, which is what is observed experimentally. Note that the surface roughness of the AlN layer for AlN/3*C*-SiC/Si(111) heterostructures grown by molecular beam epitaxy decreases with decreasing growth rate [19].

4. CONCLUSIONS

Thus, the roughness of an AlN layer grown on a SiN_x/NP-Si(100) template is 3.8 times lower than that of a layer grown on NP-Si(100) and is close to the level of roughness of AlN grown on a flat Si(111) substrate.

ACKNOWLEDGMENTS

The authors wish to thank V.K. Smirnov for providing them with NP-Si(100) substrates and T.A. Orlova for fruitful discussions.

CONFLICT OF INTEREST

The authors of this work declare that they have no conflicts of interest.

REFERENCES

1. L. Wang, W. D. Hu, J. Wang, X. D. Wang, S. W. Wang, X. S. Chen, W. Lu. Appl. Phys. Lett., **100**, 123501 (2012). https://doi.oig/10.1063/L3695154
2. Y. Taniyasu, M. Kasu, T. Makimoto. Nature, **441**, 325 (2006). https://doi.org/10.1038/nature04760
3. F. Jose, R. Ramaseshan, S. T. Sundari, S. Dash, A. K. Tyagi, M. S. R. N. Kiran, U. Ramamurty. Appl. Phys. Lett., **101**, 254102 (2012). https://doi.org/10.1063/1.4772204
4. I. S. Ezubchenko, M. Y. Chernykh, I.O. Mayboroda, I. N. Trun'kin, I. A. Chernykh, M. L. Zanaveskin. Crystallogr. Rep., **65** (1), 122 (2020). https://doi.org/10.1134/S1063774520010071
5. Y. Sun, K. Zhou, M. Feng, Z. Li, Y. Zhou, Q. Sun, J. Liu, L. Zhang, D. Li, X. Sun, D. Li, Sh. Zhang, M. Ikeda, H. Yang. Light.: Sci. Appl., **7** (1), 13 (2018). https://doi.org/10.1038/s41377-018-0008-y
6. Z.-Z. Zhang, J. Yang, D.-G. Zhao, F. Liang, P. Chen, Z.-S. Liu. Chin. Phys. B, **32** (2), 028101 (2023). https://doi.org/10.1088/1674-1056/ac6b2b
7. A. Bardhan, S. Raghavan. J. Cryst. Growth, **578**, 126418 (2022). https://doi.org/10.1016/j.jcrysgro.2021.126418
8. V. N. Bessolov, E. V. Konenkova. Tech. Phys., **68** (9), 1145 (2022). https://doi.org/10.21883/JTF.2023.09.56211.31-23

9. M. Monavarian, N. Izyumskaya, M. Muller, S. Metzner, P. Veit, N. Can, S. Das, Ü. Ozgür, F. Bertram, J. Christen, H. Morkoc, V. Avrutin. J. Appl. Phys., **119** (14), 145303 (2016). https://doi.org/10.1063/1.4945770

10. X. Luo, X. Zhang, Y. Qian, R. Fang, B. Chen, Y. Shen, Sh. Xu, J. Lyu, M.-J. Lai, G. Hu, Y. Cui. Appl. Surf. Sci., **608** (SC), 155262 (2023). https://doi.org/10.1016/j.apsusc.2022.155262

11. F. L. Riley. J. Am. Ceram. Soc., **83** (2), 245 (2000). https://doi.org/10.1111/j.1151-2916.2000.tb01182.x

12. D. du Boulay, N. Ishizawa, T. Atake, V. Streltsov, K. Furuya, F. Munakata. Acta Cryst. B, **60** (4), 388 (2004). https://doi.org/10.1107/S010876810401393X

13. V. V. Lundin, A. F. Tsatsulnikov, S. N. Rodin, A. V. Sakharov, S. O. Usov, M. I. Mitrofanov, Ya. V. Levitskii, V. P. Evtikhiev. Semiconductors, **52** (10), 1357 (2018). https://doi.org/10.21883/FTP.2018.10.46467.8861

14. V. K. Smirnov, D. S. Kibalov, O. M. Orlov, V. V. Graboshnikov. Nanotechnology, **14** (7), 709 (2003). https://doi.org/10.1088/0957-4484/14/7/304

15. V. N. Bessolov, E. V. Konenkova, T. A. Orlova, S. N. Rodin, A. V. Solomnikova. Tech. Phys., **67** (5), 609 (2022). https://doi.org/10.21883/JTF.2022.05.52376.12-22

16. W. Luo, L. Li, Zh. Li, Q. Yang, D. Zhang, X. Dong, D. Peng, L. Pan, Ch. Li, B. Liu, R. Zhong. J. Alloys Compd., **697**, 262 (2017). https://doi.org/10.1016/j.jallcom.2016.12.126

17. I. Bryan, Z. Bryan, S. Mita, A. Rice, J. Tweedie, R. Collazo, Z. Sitar. J. Cryst. Growth, **438**, 81 (2016). https://doi.org/10.1016/jjcrysgro.2015.12.022

18. L. L. Levenson, A. B. Swartzlander, A. Yahashi, H. Usui, I. Yamada. J. Vac. Sci. Technol. A, **8**, 1447 (1990). https://doi.org/10.1116/1.576855

19. A. V. Babaeva, V. K. Nevolin, V. N. Statsenko, S. D. Fedotova, K. A. Tsarik. Mech. Solids, **55**, 84 (2020). https://doi.org/10.31857/S0572329920010043

Translated by D. Safin